# Mesoscopic dots as collective terahertz oscillators

C. Metzner
*Institut für Technische Physik I, Universität Erlangen, Erwin-Rommel-Str-1, D91058 Erlangen, Germany*

D. Stehr
*Institut für Ionenstrahlphysik und Materialforschung, Forschungszentrum Rossendorf, P.O. Box 510119, D01314 Dresden, Germany*
(Received 28 June 2004; revised manuscript received 23 August 2004; published 29 November 2004)

Electrons confined in a flat semiconductor quantum dot with a parabolic in-plane potential act like a collective many-particle oscillator under coherent intraband excitation. We investigate theoretically the properties of these oscillators under a simultaneous scale transformation of the lateral dimensions and the electron occupation number. As the lateral size increases from a few nm (typical for self-assembled dots) to the mesoscopic regime, the physics of the system is changing qualitatively: Quantization effects gradually lose importance against Coulomb interactions and eventually the electron lake in a mesoscopic dot resembles a classical Wigner liquid. This parabolically confined "Wigner lake" behaves to the outside like a form-elastic "superparticle" of high charge. It can be coherently controlled by THz dipole radiation just like a single electron, but with reduced Brownian diffusion in the phonon heat bath. We propose a flexible method to fabricate single mesoscopic dots of a controlled shape, Coulomb-coupled groups of dots, and almost arbitrary potential landscapes, using current semiconductor technology. As a first example, the collective modes of two Coulomb-coupled superparticles in neighboring dots are calculated. Also, we consider the possibility of steering a superparticle with shaped laser pulses to follow any complex two-dimensional orbit.

DOI: 10.1103/PhysRevB.70.195433 PACS number(s): 73.21.−b, 78.67.−n, 78.47.+p

## I. INTRODUCTION

### A. Quantum dots

The name "quantum dot" implies a zero-dimensional system with strong size quantization—i.e., with spatial dimensions smaller than the de Broglie wavelength of the confined electrons and holes. At present, the most prominent and widely studied examples in the semiconductor community are probably self-assembled dots (SAD's). These are usually flat, lenslike objects with a lateral size of several 10 nm and a height of a few nm, which can to a good approximation be described by parabolic in-plane confinement potentials. They typically host fewer than ten particles and have quantized level spacings around 50 meV. The scientific work on these systems is mainly focused on their optical interband properties, as for example PL spectra.

The self-organized growth of quantum dots is certainly elegant and convenient. However, it is not possible with this approach to fully control the resulting effective confinement potential, in the sense that one could create arbitrary potential landscapes (as has long been possible for simple layered systems like multiple quantum wells). Therefore it is also difficult to build more complex systems on the basis of SAD's as elementary building blocks. For example, the most natural extension of an "artificial atom," a coupled quantum dot molecule, can be formed in a vertically stacked configuration using strain fields. But to achieve lateral coupling (in the form of interdot tunneling or at least via Coulomb fields) would be extremely difficult. The main obstacle for realizing this and other interesting many-dot systems (like ordered lateral arrays of Coulomb coupled dots with collective optical modes) is the huge interdot spacings compared to the short effective range of the induced Coulomb fields of the dots.

Historically, the first quantum dot structures were not self-assembled, but fabricated in a controllable technological process. Normally one started from a burried two-dimensional (2D) electron gas, which provided the longitudinal confinement. Then, the lateral confinement was either achieved by etching a free-standing pillar[1,2] or by superposing an electrostatic lateral confinement field. The latter was typically created by some modulated gate electrode, which at the same time allowed precise tuning of the electronic occupation of the dot.[3–5] With both approaches, huge periodic dot arrays could be fabricated. Often, again, the effective in-plane potential of each dot was parabolic to a good approximation.

These "old" type of dots had a comparatively weak confinement with typical level spacings $<10$ meV and could be occupied by a relatively large number of electrons, but not simultaneously by holes. Naturally, the investigations then concentrated on the intraband excitations of these systems in the far-infrared (FIR) regime, frequently combined with longitudinal magnetic fields, in order to enhance the lateral confinement. It was, however, quickly discovered that the optical spectra show almost no dependence on the electron number in each dot.[3] The reason was found in the generalized Kohn theorem.[6–8] It states that, in the special case of parabolic lateral potentials, the only collective dipole resonances are rigid center-of-mass motions of the electron gas as a whole, and those have the same absorption spectrum as a single electron. This result seems to have been received with a certain disappointment in the community. Thus, with the time the main focus of interest moved to electron-hole complexes in SAD's with a strong size quantization, in which many-body effects are more significant and spectra *do* depend (to a certain degree) on the particle numbers.

 

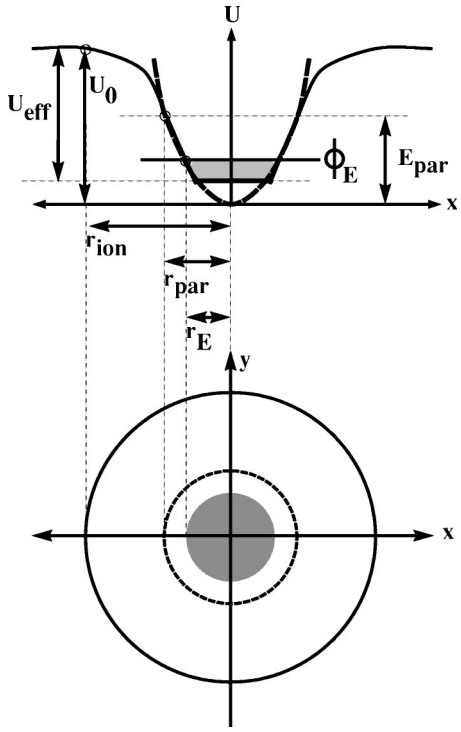


FIG. 1. Schematic drawing of the lateral potential well of a rotationally symmetric quantum dot. The upper part shows the screened potential profile (solid line) versus the $x$ coordinate, together with a parabolic approximation (dashed line) of the bare potential. The lower part depicts some characteristic equipotential lines in the $x$-$y$ plane. The shaded region corresponds to the area occupied by electrons.

### B. Mesodots

In this paper, the case of weak confinement (large size) and high electronic (no holes) occupation is reconsidered. We shall call such systems mesoscopic dots or "mesodots." As their lateral size is growing from nanoscopic (several 10 nm) to mesoscopic (0.1–1 $\mu$m), the physics is altered in qualitative ways, providing interesting opportunities for both fundamental investigations and new applications.

To see this, consider a 2D rotationally symmetric potential well $U(r)$ of Gaussian-like shape (compare Fig. 1). Assume the potential is parabolic ($U=\alpha r^2$) for radii $r<r_{par}$, flattens out for $r\geqslant r_{par}$, and becomes essentially zero for $r\geqslant r_{ion}$. With one or more electrons bound in the well, the system represents an optical *oscillator* for in-plane polarized light, with a harmonical response for sufficiently weak excitation.

As we shall demonstrate in detail later on, the whole packet of bound electrons can move collectively and without dispersion in a parabolic potential as a compact *superparticle* of giant charge $Q$.[9] In practice, the number $N_E$ of electrons that can be added to this superparticle is limited, because eventually its growing radius $r_E$ becomes comparable to the width $r_{par}$ of the parabolic regime. At this point, the Fermi energy $\Phi_E$ is equal to the "maximum parabolic energy" $E_{par}=\alpha r_{par}^2$ of the well.

How are the properties of this superoscillator changing when its spatial dimensions are scaled up by a factor $s$—i.e., under the transformation $r\rightarrow r/s$? Primarily, the lateral stretching widens the parabolic regime and reduces the effective curvature $2\alpha$ of the potential, which in turn *lowers the resonance frequency* $\omega_0$ of the harmonic oscillator. In the quantum regime, the spacing $\epsilon_{10}=\hbar\omega_0$ of the energy ladder is decreasing until *size quantization is no longer the dominating factor* of the system.

With the energetic density of levels thus growing, a larger number $N_E$ of electrons can be added to the well before $\Phi_E$ reaches $E_{par}$. Since the potential profile is also smoothened by the spatial stretching transformation, a classical description of these particles becomes applicable even for relatively low kinetic energies. In other words, *the scaled-up dot can host a larger superparticle and undergoes a gradual transition from the quantum to the (semi)classical regime*.

When excited with resonant laser light of circular in-plane polarization, the superparticle will orbit around the dot center like in a cyclotron. In the stationary state, the external driving field will just compensate for the energy losses due to the (mainly coherent) emission of phonons and electromagnetic radiation. The radius $r_{orb}$ of the orbit then depends on the effective relaxation time $\tau$ and the laser field strength $E_0$. However, if we consider these quantities as fixed, *the orbital radius* $r_{orb}$ *increases with the scaling parameter* $s$.

Combined with the huge charge $Q=N_E e$ of the superparticle, its large orbital radius $r_{orb}$ leads to an *extremely good polarizability* $Qr_{orb}/E_0$ *of the oscillator*. Due to the *superradiance effect* of the $N_E$ electrons oscillating in phase, it will therefore *emit a high power of coherent radiation*, which should be relatively easy to detect experimentally.

But also in the optical near field close to the dot, the ac electric fields induced by the charge oscillation will be much stronger compared to typical SAD systems. This enables a *significant Coulomb interaction between neighboring mesodots* and opens the way to coupled oscillator networks and optically active regular dot arrays.

High polarizability also means that it is possible to drive the oscillator with relatively small laser fields into the nonharmonic regime.[10] Such a system is therefore also ideally *suited for nonlinear optical experiments*, including effects like higher and subharmonic generation or multistability.

In the extreme case, it becomes possible to achieve a *complete ionization* of the oscillator, once $r_{orb}>r_{ion}$. As we shall show later, one can also think of coherent control experiments in which the superparticle is transferred all optically from one mesodot to a close by neighbor and then stays there in a metastable state until it is transferred back by another shaped laser pulse.

Compared, for example, to coherent control of Rydberg atoms, the mesodot system fundamentally suffers from very short decoherence times (often in the sub-ps scale), due to the efficient electron-phonon coupling in the semiconductor matrix. However, using nonresonant circular polarized excitation, it is possible in principle to control the radius $r_{orb}$ and orbital velocity $v_{orb}$ of the superparticle independently from each other. In this way, the kinetic energy $E_{kin}=(m^*/2)v_{orb}^2$ can always be kept below the threshold $E_{LO}$ for LO phonon emission,[11] thus effectively turning off this scattering channel.[12] It has been shown that in wide quantum wells, where the quantization energy $\epsilon_{10}$ is below $E_{LO}$, the relax-

ation times $\tau$ increase dramatically (up to almost 1 ns), provided the electron temperature is also kept low (see Ref. 13 and references therein).

In addition, we will demonstrate later that the center-of-mass motion of the superparticle intrinsically has smaller Brownian velocity fluctuations than that of a single constituent electron. In combination, these features suggest that superparticles in mesodots are *well suited for coherent control* and that these systems can have a *very high oscillator quality*.

Finally, we would like to mention a practically important advantage connected with the larger size of mesodots: They are in a *range accessible by modern semiconductor fabrication techniques* (compare section below), which allow a spatially selective control of the sample properties in the lateral dimension. On the mesoscopic scale, it is possible to create practically *arbitrary lateral potential landscapes*, like configurations of different potential valleys and connecting channels. In the future, it might therefore even become possible to perform coherent control experiments of a complexity comparable to those in the field of "femtochemistry" with complex molecules.

The paper will be organized as follows: In the following section, we will propose methods for the fabrication of mesodot systems. Then the properties of these systems will be quantitatively investigated in a simple analytical model. Finally, we will summarize and discuss some of the future prospects.

## II. FABRICATION METHODS

As in the case of the "old" type of quantum dots, our concept is also based on a two-dimensional quantum well, which is then turned into a zero-dimensional system by superposing a lateral confinement potential. If the well is *n*-modulation doped, it becomes occupied by electrons, leaving behind positively charged donors in the impurity layer. Due to statistical fluctuations of the local doping concentration, the Coulomb potential $U(x,y,z)$ of these charged donors is never completely homogeneous in the lateral $(x,y)$ directions, but fluctuates randomly around some average value $\overline{U}(z)$. For finite (but not too large) spacer layer thicknesses $d$, only the long-wavelength Fourier components $\lambda \geqslant d$ of the potential fluctuations are transmitted to the quantum well plane. This leads to a smooth lateral potential landscape of hills and valleys, which are approximately parabolic around the extremal points.

The electrons in the quantum well are attracted by the local potential minima and will develop density maxima at these lateral positions. Normally, the Fermi level is located at energies above the highest hills of the potential landscape and thus the electron density is only weakly modulated. However, in the case of extreme potential fluctuations the electron sea will desintegrate into spatially isolated "lakes" and, thereby, natural quantum dots are formed. While this disorder-induced localization of the electron sea (accompanied by a metal-insulator transition) is unwanted for most applications, we propose to use this effect purposefully for the generation of designable in-plane potential landscapes.

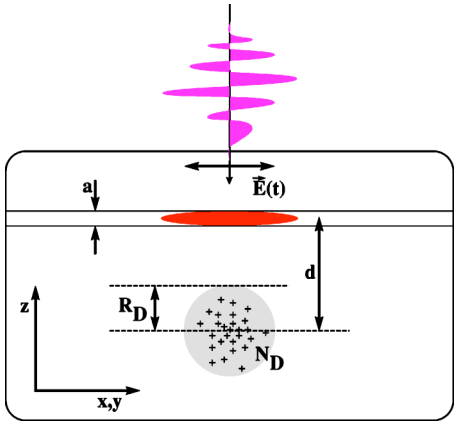


FIG. 2. (Color online) Schematic sample structure of a mesoscopic dot in the "doping ball model." The figure shows (along the growth coordinate $z$ running from bottom to top) the doping ball with the positively charged donors, the longitudinal quantum well with the 3D confined electrons and a light pulse, seen as a time-dependent electric field.

For this purpose, it is required to control the spatial fluctuations of the local donor density in the remote impurity layer. Such a spatially selective doping method is indeed available since several years with the focused ion beam (FIB) technique.[14,15] It allows to control the doping density laterally on a scale of less than 100 nm. In the case of *n* doping with Si ions, the implantation profile in the longitudinal direction (along the beam) depends on parameters like the ion acceleration voltage and the beam current.[16,17] With a proper choice, the width of the bell-curve-shaped ion distribution can also be reduced to the order of 100 nm. In principle, one can thus write arbitrary 3D doping patterns within the limits of this spatial resolution.[18–21]

In the simplest case, the FIB method allows us to concentrate all the donors in a bounded region of mesoscopic size $R_D$ at distance $d$ from the quantum well (compare Fig. 2). This leads to the formation of a single mesoscopic quantum dot with tunable properties, as will be shown in the following section. Note that due to the suppression of short-range potential fluctuations by the spacer layer, the resulting lateral potential minimum in the well is rather robust against variations of the doping concentration on an atomic scale.[22]

## III. THEORY AND RESULTS

### A. Doping ball model

Let us start thus with a 2D quantum film in the $z=0$ plane of a host semiconductor matrix, defined by a narrow rectangular potential well of width $a$ in the electric quantum limit.[23] Assume, for simplicity, that all donors are contained in a sphere of radius $R_D$, centered at a distance $d>R_D$ away from the well at position $(x=0,\ y=0,\ z=-d)$ (compare Fig. 2). If the density distribution $n_D(\vec{R})$ of the charged dopands is 3D rotationally symmetric within the sphere ("doping ball model"), they produce a Coulomb potential which appears from the outside like that of a single point charge $Q_D = e\int n_D(\vec{R})d^3R = eN_D$.

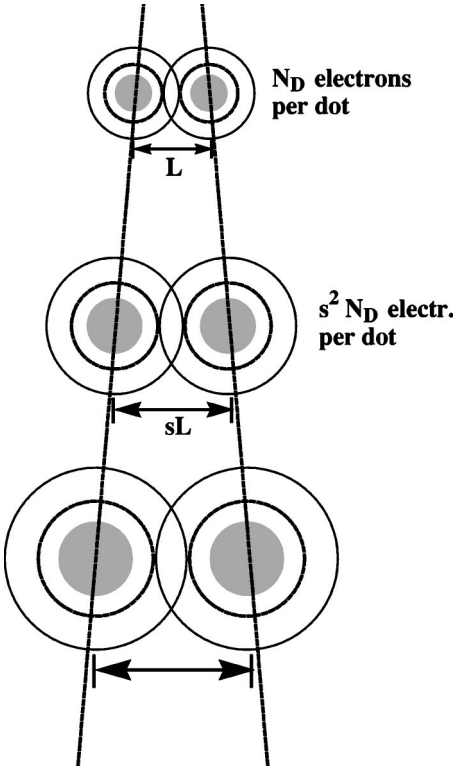


FIG. 3. Schematic diagram, depicting the simultanenous scaling of the spatial size and electronic occupation number for a pair of mesoscopic dots.

### B. Mesodot potential

In particular, the potential profile $U(x,y)=U(\vec{r})=U(r)$ created in the quantum well plane at $z=0$ is given by

$$U(r)=\frac{-e^2N_D}{4\pi\epsilon_0\epsilon_r\sqrt{r^2+d^2}}=\frac{-N_Dk_0}{\sqrt{r^2+d^2}}, \tag{1}$$

where $\epsilon_r$ is the static dielectric constant and $k_0$ a convenient abbreviation used frequently in the following. The full width at half maximum $l$ of this in-plane potential well is $l=\sqrt{3}d$. Here, we are primarily interested in the mesoscopic limit, where $d\gg a$, with $d$ lying somewhere in the $\mu$m and $a$ in the nm range. By combining the weak lateral Coulomb well with the tight longitudinal confinement of the quantum film, one obtains a "mesodot" with tunable properties. As can be seen in Fig. 1, the Coulomb well is parabolic for small deviations from the minimum—i.e., $U(r<r_{par})\approx\alpha r^2$, with $r_{par}\approx 0.4d$. (At $r=r_{par}$ the relative error is smaller than 1% and grows at $r=d$ to around 29%.) The depth $U_0=|U(r=0)|=N_Dk_0/d$ and curvature $2\alpha=N_Dk_0/d^3$ can be controlled independently by a proper choice of the two design parameters $N_D$ and $d$.

### C. Dot scaling

In the following we will repeatedly consider a simultaneous scaling of the spatial size and electron occupation number of the dots (compare Fig. 3). Within the framework of the doping ball model, this is achieved by the simple design parameter transformations $d\to sd$ and $N_D\to s^2N_D$. As a consequence, all the Coulomb-related energies, in particular the depth $U_0$ of the unscreened potential well, grow linearly with the scaling factor or $U_0\to sU_0$. The curvature of the parabola, on the contrary, is reduced by the lateral stretching, with $\alpha\to\alpha/s$.

We numerically evaluate the scaling behavior of the doping ball model for the case of the GaAs/AlGaAs semiconductor system, using an effective electron mass of $m^\star=0.065m_0$ and a relative dielectric constant of $\epsilon_r=12.7$. The scaling is started at $s=1$ with only one donor ($N_D=1$) placed at a distance of $d=10$ nm from the quantum well. Under these conditions, the lateral well has a small depth of $U_0=11.3$ meV and hosts a single electron (with significant size quantization). The scaling parameter $s$ is then increased from 1 to 100. In the final setting, there are $N_D=10^4$ electrons in a mesoscopic dot of size $d=1$ $\mu$m and depth $U_0=1.13$ eV. Our main range of interest is located in between these extreme cases.

### D. Classical regime

Electrons propagating with high kinetic energy $E$ in a smooth potential landscape are expected to behave like classical particles. A condition for this quasiclassical regime is that many de Broglie wavelengths $\lambda_{DB}(E)=2\pi\hbar/\sqrt{2m^\star E}$ fit into the linear dimension $l(E)$ of the spatial region which is classically accessible to the particle—i.e., where $E>U(\vec{r})$. In a parabolic potential $U=\alpha r^2$ at energy $E$, this accessible length scale $l$ can be estimated by $U(l/2)=E$, yielding $l(E)=s\sqrt{E/\alpha}$. For the ratio we obtain $l/\lambda_{DB}=[2m^\star/(\pi^2\hbar^2)]^{1/2}\alpha^{-1/2}E$. We require that $(l/\lambda_{DB})\gg 1$ in the classical regime; i.e., there exists a minimum kinetic energy for a particle to behave classical. Since the ratio scales like $\sqrt{s}E$, we find that in the limit of large $s$ this minimum energy tends towards zero: Mesodots are classical systems.

### E. Single-particle oscillator

Next consider a single electron of effective mass $m^\star$ and charge $q=-e$ in the mesodot. In the electric quantum limit, its dynamics is restricted to lateral motions $\vec{r}(t)=(x(t),y(t))$ parallel to the quantum film. Due to the smooth lateral potential, we can describe this lateral dynamics classically on the basis of Newton's laws of mechanics. The electron experiences a confinement force $\vec{F}_{cnf}=-\nabla U(\vec{r})$, which is harmonic in the parabolic region, $\vec{F}_{cnf}(r<r_{par})=-2\alpha\vec{r}$. This 2D oscillator has a classical eigenfrequency (or resonance frequency) $\omega_0=\sqrt{2\alpha/m^\star}$, with a scaling behavior of $\omega_0\to\omega_0/\sqrt{s}$.

In the semiconductor matrix, the electron will experience additional coupling to the phonon heat bath, in the form of statistical scattering events, which change the direction and modulus of the electron momentum. For the purpose of this simple analytical investigation, we shall for the time being ignore the fluctuating part of the electron-phonon interaction and retain only an average deterministic friction force proportional to the velocity, $\vec{F}_{fri}=-2\gamma\dot{\vec{r}}$, where $2\gamma=m^\star/\tau$ and $\tau$ is an empirical relaxation time. This force will also provide

relaxation of the electron to the stable equilibrium position in the dot center.

In addition, the electron will be controlled by external coherent radiation. Typically, this radiation will propagate along the longitudinal ($z$) direction and be linearly or circularly polarized in the film plane. In our classical model, light is described as a time-dependent electric field $\vec{E}(t)$, acting on the electron with a force $\vec{F}_{ext}=q\vec{E}(t)$. For resonant optical excitation of a typical mesoscopically sized dot, the light field must have relatively low photon energies $E_{phot}=\hbar\omega_0$ in the range of a few meV, which belongs to the THz regime.

The dipole approximation for the electron-light interaction is applicable under the condition that the wavelength $\lambda=2\pi(c_0/\sqrt{\epsilon_r})/\omega_0$ be large compared to the typical size of the system, which is given by $d$ in the doping ball model. Since the ratio $\lambda/d$ scales like $1/\sqrt{s}$, the dipole approximation would eventually break down in the limit of extremely large dot sizes. However, this happens beyond our regime of interest.

For arbitrary control fields $\vec{E}(t)$, the electron dynamics follows from $m^\star\ddot{\vec{r}}=\vec{F}_{cnf}+\vec{F}_{fri}+\vec{F}_{ext}$. For stationary monochromatic excitation with light polarized in the $x$ direction, $\vec{E}(t)=\vec{e}_xE_0\cos\omega t$, the oscillating $x$ position of the particle is given by $x(t)=qE_0\,\mathrm{Re}\{R(\omega)e^{i\omega t}\}$. Here $R(\omega)=1/[m^\star(\omega_0^2-\omega^2)+im^\star(\omega/\tau)]$ is the complex-frequency-dependent response function. The induced amplitude of the electron oscillation is $\Delta x(\omega)=qE_0|R(\omega)|$. In the static limit ($\omega=0$) one obtains $\Delta x(0)=qE_0/(m^\star\omega_0^2)$, which grows linearly as a function of the scaling parameter, $\Delta x(0)\to s\Delta x(0)$; i.e., this quantity is stretched together with the characteristic dimensions of the potential. At resonance ($\omega=\omega_0$), the amplitude depends on the relaxation time as $\Delta x(\omega_0)=qE_0\tau/(m^\star\omega_0)$. This dynamic amplitude is only proportional to $\sqrt{s}$, but one should keep in mind that in the mesoscopic regime we expect much longer relaxation times $\tau$. Note also that the polarizability of the oscillator is $N_Dq\Delta x/E_0$ (scaling like $s^3$ in the static and like $s^{5/2}$ in the dynamic case). Its quality factor is $\mathcal{Q}=\Delta x(\omega_0)/\Delta x(0)=\omega_0\tau$.

We can define a critical electric field strength $E_{NL}$ for resonant light, at which the oscillating particle starts to transgress the limit $r_{par}$ of the parabolic confinement region, $E_{NL}=m^\star\omega_0r_{par}/(q\tau)$. This corresponds to a radiation power density of $(P/A)_{NL}=(c_0\epsilon_0\sqrt{\epsilon_r})E_{NL}^2$. For stronger fields, we expect nonlinear effects in the optical properties of the oscillator.

### F. Electron lake

Under the condition that the conduction band (CB) edge at the dot center ($x=0$, $y=0$, $z=0$) be sufficiently low compared to the doped barrier region, all $N_D$ donors in the doping ball inject their electrons into the dot. However, for many applications it will be useful if the electron occupation number $N_E$ of the dot can be tuned between zero and its maximum possible value $N_D$.[24] We thus define a dimensionless *filling factor* $f=N_E/N_D$, which varies between 0 and 1.

The $N_E$ mobile particles will then collect around the dot center and form there an electron "lake." The equilibrium density distribution $n^{(2)}(\vec{r})$ and lateral radius $r_E$ of the lake are determined by a balance between the compressive confinement force $F_{cnf}=-2\alpha r$ and the expansive forces due to temperature, Coulomb repulsion, and the "Fermi pressure" (related to the Pauli principle for an electron gas in the degenerate limit, when the Fermi level $\Phi_E$ is greater or comparable to $k_BT$). In the following, we will roughly estimate these three contributions, occasionally using simple scaling arguments.

At high temperature—i.e., in the nondegenerate limit when $k_BT\gg\Phi_E$—the particles will obey a Boltzmann statistics. Then, in our two-dimensional system with parabolic in-plane confinement and neglecting screening, the density distribution of the electrons is Gaussian, $n^{(2)}(r)=n_0^{(2)}e^{-(r/r_T)^2}$ with a spatial spread $r_T=\sqrt{k_BT/\alpha}$ independent from the particle number $N_E$. Note that the thermal lake radius $r_T$ for a given confinement parameter $\alpha$ can be reduced arbitrarily by lowering the temperature.

The Coulomb repulsion force can be estimated as follows: If, in the equilibrium situation, all electrons are confined within a disk of radius $r_E$, the mean interparticle distance is of the same order. Thus the magnitude of the (radially outward directed) Coulomb force on a particle at the border of the lake (at radius $r_E$) should scale like $|F_{Coul}|=\eta^3(N_E-1)k_0/r_E^2$, where $\eta^3$ is a dimensionless geometry factor of order 1. Equating $F_{Coul}$ with the inward-directed confinement force $|F_{cnf}|=2\alpha r_E$ yields in the limit of many particles $r_E=\eta(k_0N_E/2\alpha)^{1/3}$.

The corresponding potential Coulomb energy is $E_{Coul}=k_0N_E/r_E$. This is also the amount by which the screened potential well is flatter than the bare well without electrons (see Fig. 1); i.e., the effective depth is $U_{eff}(N_E)=U_0-E_{Coul}$ and it becomes zero at a maximum filling factor of $f_{max}=\eta^{3/2}$.

In the doping ball model, we can express $2\alpha$ by the design parameters $2\alpha=k_0N_D/d^3$ and find that $r_E=\eta f^{1/3}d$. Numerical simulations (see later) confirm this scaling relation and show that $\eta$ is indeed of order unity. Note that with $r_E\approx d$, the outer electrons would already be located beyond the strictly parabolic confinement region. To avoid this, it is required to work with filling factors smaller than 1.

Next, we compute the Fermi energy $\Phi_E$ of the degenerate electron gas, relative to the potential of the screened well at its center. From numerical simulations we find that on a scale of $U_0$ the screened potential well is essentially flat in the region $r\leqslant r_E$ and then increases steeply for $r>r_E$. As a simple approximation, we can therefore assume that the interacting electrons self-consistently "feel" a disklike confinement potential (compare Fig. 1). Neglecting size quantization effects for the large spatial scales we are interested in, we can assign a constant 2D density of states $D^{(2)}=m^\star/(\pi\hbar^2)$ to each space-energy element within the disk. Since the spatial area of the disk is $\pi r_E^2$ and its energetic "height" is given by the Fermi energy $\Phi_E$, the number $N_E$ of electrons in the disk is $N_E=\Phi_E(m^\star/(\pi\hbar^2))(\pi r_E^2)$. This yields a Fermi energy of $\Phi_E=(\pi\hbar^2/m^\star)N_E/(\pi r_E^2)=(\pi\hbar^2/m^\star)n_{av}^{(2)}$, where $n_{av}^{(2)}$ is the average 2D electron density in the lake.

Let us now consider the scaling behavior of the above quantities. First we note that with $r_E=\eta f^{1/3}d$, the radius of

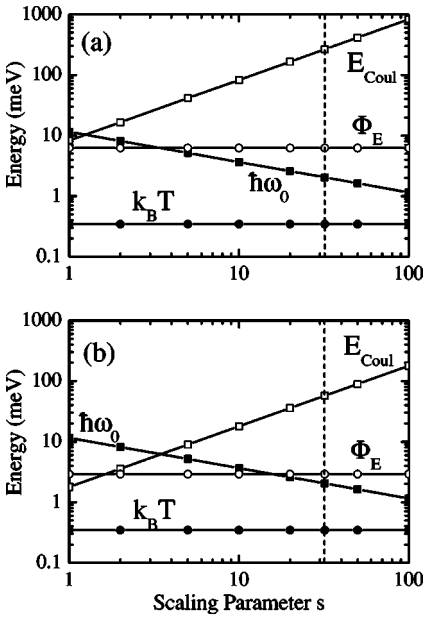


FIG. 4. Double-logarithmic plot of the various characteristic energies versus the scaling parameter $s$. (a) Corresponds to filling factor $f=1$, (b) to $f=0.1$. The dashed vertical line marks the case $s=32$.

the electron lake at fixed filling factor grows in proportion with the other spatial dimensions, $r_E \to s r_E$. Since $N_E$ increases quadratically with $s$, the average 2D density of electrons in the lake remains asymptotically constant, $n_{av}^{(2)} = \text{const}$, and the same holds for the Fermi energy, $\Phi_E = \text{const}$.

The Coulomb energy $E_{Coul} = k_0 N_E / r_E$, on the other hand, scales linearly with $s$. Therefore, in the mesoscopic regime, it will be the Coulomb effects that determine the physics of the electron gas. We can calculate the critical lake radius $r_C$ at which the Coulomb and Fermi energies become equal. This yields $r_C = \hbar^2/(k_0 m^\star) = a_0$; i.e., the transition to the Coulomb-dominated regime occurs as soon as the lake radius exceeds the effective Bohr radius $a_0$ of the system.

Note that $\Phi_E$ can also be interpreted as a measure of the kinetic energy of the electrons and $E_{Coul}$ as the typical potential energy of the interaction. In the limit $E_{Coul} \gg \Phi_E$, we expect a phase transition from a gaseous to a liquid or solid state of the many-particle system. We have also seen above that the system can be described classically for sufficiently large $s$. At zero temperature, the electron lake will thus form a classical Wigner crystal, where all particles arrange in a triangular lattice. (The lattice constant in the center of the lake will be smaller than at its border, because of the confinement of the lake. A quantum mechanical study of Wigner crystallization for small particle numbers can be found, e.g., in Refs. 25 and 26.) At higher temperatures the crystal will melt and resemble a Wigner liquid, but still with pronounced interparticle correlations.

In the double-logarithmic plots of Fig. 4 we show how the various characteristic energies scale with $s$, for filling factors $f=1$ and $f=0.1$, respectively. We have also included the resonance photon energy of the oscillator, $\hbar\omega_0 = \hbar\sqrt{2\alpha/m^\star} \propto s^{-1/2}$, and the thermal energy at $T=4$ K. For $s<4$ or so, the Coulomb and Fermi energies are still of comparable magnitude. However, if we choose, for instance, $s=32$, we have an interesting physical situation: The thermal energy is an order of magnitude below $\Phi_E$, while $E_{Coul}$ is more than one order higher than $\Phi_E$; i.e., this should correspond to the Wigner crystal regime. At a filling factor of $f=0.1$ (which guarantees that all electrons are in the parabolic regime), one would have about 100 electrons in a Wigner lake of radius 0.2 $\mu$m, absorbing at a photon energy of about 2 meV (corresponding to a frequency of 0.5 THz and a wavelength of 0.17 mm). The case $s=32$ is realized with design parameters $N_D = 1024$ and $d=0.32$ $\mu$m, which is feasible with standard FIB technology. (The number $N_D$ of donors in the doping ball corresponds, for example, to a ball radius of 0.1 $\mu$m and inside the ball to a homogeneous doping density of $N_D^{(3)} = 2.45 \times 10^{17}$ cm$^{-3}$).

The analysis above thus leads to the following conclusion: In the limit of low temperature, weak confinement, and large particle number (large scaling parameter $s$), the density distribution and radius of the electron lake are mainly determined by the Coulomb repulsion between the electrons. The situation then corresponds to a confined classical Wigner crystal at zero temperature and to a Wigner liquid at higher temperatures. Asymptotically, the Coulomb energy and the lake radius grow linearly with $s$, while the average 2D electron density and Fermi energy remain constant.

### G. Screened potential

In order to check the above scaling relations, we have performed two different kinds of numerical simulations of the mesoscopic electron lake under 2D parabolic confinement, assuming low temperature and zero thickness of the system in the longitudinal direction $z$.

The first calculation is based on a semiclassical continuum model. It describes the system by 2D rotationally symmetric profiles of the electron density $n^{(2)}(\vec{r})$ and the total (screened) potential $V_{scr}(\vec{r}) = U(\vec{r}) + V(\vec{r})$. Here, $U$ is the unscreened lateral potential well and $V$ is the Hartree contribution, which results via Poisson's equation from the 3D charge distribution $\rho^{(3)}(\vec{R}) = (-e) n^{(2)}(\vec{r}) \delta(z-0)$. In accordance with our mesoscopic regime of interest, the electron density was computed semiclassically (neglecting size quantization effects), assuming locally the constant density of states of a 2D system. This yields $n^{(2)}(\vec{r}) = [m^\star/(\pi\hbar^2)] \int dE\, \theta(E - V_{scr}(\vec{r}))\, f((\Phi_E - E)/(k_B T))$, where $\theta(x)$ is the Heaviside step function and $f(x) = 1/(1+e^x)$ the Fermi function. For a given total number of electrons, $N_E = \int n^{(2)}(\vec{r}) d^2 r$, the Fermi level $\Phi_E$, density profile $n^{(2)}(\vec{r})$, and total screened potential $V_{scr}(\vec{r})$ have been determined self-consistently.

For the calculation we chose a parabolic potential of curvature $2\alpha = N_D k_0 / d^3$, with design parameters $N_D = 100$ and $d = 0.1$ $\mu$m, corresponding to a scaling variable of $s=10$. The resulting screened potentials $V_{scr}(r)$ for various electron filling factors $f = 0.0, 0.2, 0.4, 0.6, 0.8, 1.0$ are plotted in Fig. 5. One can clearly see that the self-consistent well is flat at the bottom of the electron lake and increases quadratically for $r > r_E$. The inset shows the Coulomb energies $E_{Coul}$ [corresponding also to $V_{scr}(\vec{r}=\vec{0})$] as a function of electron number

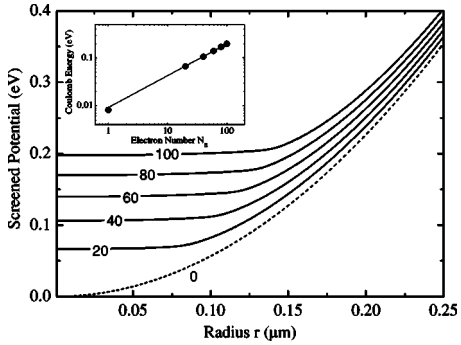


FIG. 5. Self-consistent potentials (solid lines) and bare potential (dashed line) of a parabolic lateral confinement, correponding to a mesodot with scaling parameter $s=10$. The numbers (0, 20, 40, 60, 80, and 100) denote the respective electron numbers $N_E$. The inset is a double-logarithmic plot of the Coulomb energy (screened potential at $r=0$) versus electron number (dots), compared to the analytic relation (solid line, $\eta=0.575$).

$N_E$ in a double-logarithmic plot, together with the analytic scaling relation for a fitted geometry factor of $\eta=0.575$. Figure 6 depicts the radial dependence of the electron density profiles $n^{(2)}(r)$ for the same parameters as in Fig. 5. Note that if the bottom of the lake were really perfectly flat, the electron density would be constant. Actually, the screened well is only approximately flat on a scale of $E_{Coul}$ (or $U_0$), but slightly increases with radius $r$. Thus the corresponding density profile drops continuously from a maximum at the well center to zero at the border of the lake. The inset shows the lake radius versus electron number in a double-logarithmic plot, confirming the analytic scaling relation. There is a constant factor between the simulated and analytic data, due to the somewhat arbitrary definition of the lake radius.

In the second type of simulation, the $N_E$ electrons were described completely classically as point particles with repulsive Coulomb interactions, subject also to the radial forces of the lateral potential well and to friction forces proportional to the velocity. The temperature was assumed zero. Since the equilibrium electron lake is a "fixed point" of the dissipative dynamical system, we defined some random ini-

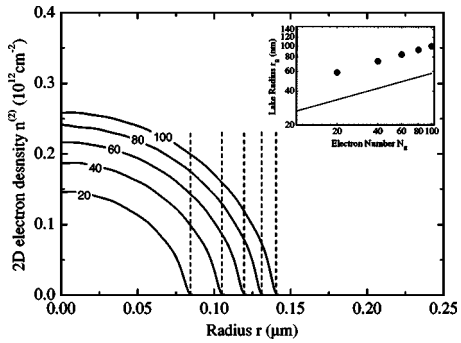


FIG. 6. Electron density profiles, corresponding to the self-consistent potentials of Fig. 5. The vertical dashed lines mark the "shore" of the electron lake. The inset is a double-logarithmic plot of the lake radius (determined fromthe shore lines) versus electron number (dots), compared to the analytic relation (solid line, $\eta=0.575$).

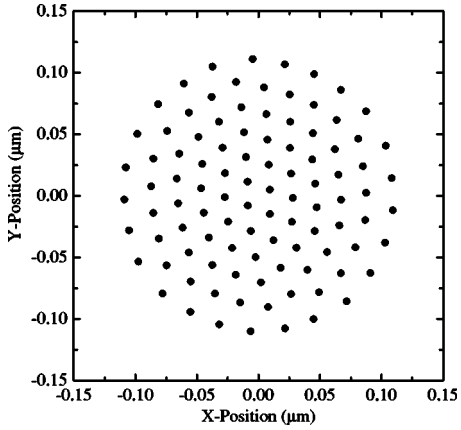


FIG. 7. Stable equilibrium configuration of 100 classical electrons in a parabolic lateral confinement, corresponding to the same situation as in Figs. 5 and 6 for $N_E=100$.

tial positions and velocities for the particles and then simply let them relax, according to Newton's laws.[27] As expected, the particles "self-organize" into the highly correlated Wigner lattice state independently from the initial conditions.

The simulation was performed for the same parameters as in Figs. 5 and 6. As a typical example of the resulting equilibrium particle configuration, we present in Fig. 7 the case of $N_E=100$. One finds a triangular lattice order and a particle density that decrease from the center to the shore of the electron lake. We have determined the lake radii as a function of the particle number and again confirmed the $r_E \propto N_E^{1/3}$ relation.

### H. Superparticle concept

Parabolic potentials are peculiar in many respects and some of their specific properties are connected with the (generalized) Kohn theorem. Although this theorem and its consequences have already been discussed in various publications, we will reconsider it in the following for our classical mesodot system.

The Hamilton function of the isolated[28] interacting $N$-electron system in the parabolic confinement region reads

$$H=\sum_{i=1}^{N}\frac{(\vec{p}_i)^2}{2m^\star}+\sum_i\frac{m^\star\omega_0^2}{2}(\vec{r}_i)^2+\frac{1}{2}\sum_{i,j}V(\vec{r}_i-\vec{r}_j). \qquad (2)$$

The center-of-mass (c.m.) position $\vec{s}$ of the $N$ particles is given by $\vec{s}=(1/N)\Sigma_i\vec{r}_i$, their total mass by $M=Nm^\star$. We can also define relative positions $\vec{d}_{ij}=(1/N)(\vec{r}_i-\vec{r}_j)$ and, based on those, the new variables $\vec{D}_i=\Sigma_j\vec{d}_{ij}$. The quantity $\vec{D}_i$ can be interpreted as the distance vector of particle $i$ relative to the c.m., and one can easily demonstrate the property $\Sigma_i\vec{D}_i=\vec{0}$. If the original variables $\vec{r}_i$ (and $\vec{p}_i=m^\star\dot{\vec{r}}_i$) in our Hamilton function are replaced by $\vec{r}_i=\vec{s}+\vec{D}_i$ (and $\vec{p}_i=m^\star\dot{\vec{s}}+m^\star\dot{\vec{D}}_i=\vec{p}_s+m^\star\dot{\vec{D}}_i$, respectively), one obtains

$$H = H_{com} + H_{rel} + H_{ee} = \left[ \frac{(\vec{p}_s)^2}{2M} + \frac{M\omega_0^2}{2}(\vec{s})^2 \right] + \sum_i \left[ \frac{m^\star}{2}(\dot{\vec{D}}_i)^2 + \frac{m^\star\omega_0^2}{2}(\vec{D}_i)^2 \right] + \left[ \frac{1}{2}\sum_{i,j} V(N\vec{d}_{ij}) \right]. \tag{3}$$

This shows, first, that the center of mass and relative degrees of freedom of the interacting $N$-particle system are completely decoupled in the case of a parabolic confinement. Second, the Coulomb interactions affect the relative coordinates $\vec{d}_{ij}$ only.

This separation is also possible in the presence of friction forces. For example, the friction force on the $i$th particle can be written as a sum of two parts, $\vec{F}_{fri}^{(i)} = -2\gamma\dot{\vec{r}}_i = -2\gamma\dot{\vec{s}} - 2\gamma\dot{\vec{D}}_i$.

We now reinclude the external dipole radiation, which we have described by a time-dependent electric field $\vec{E}(t)$. The corresponding term in the Hamilton function reads $H_{ext} = -q\vec{E}\Sigma_i\vec{r}_i$. Performing again the above variable transformation, we obtain $H_{ext} = -Q\vec{E}\vec{s}$, where $Q = Nq$ is the total charge of the $N$ electrons. Since the electric field is spatially homogeneous, it simultaneously and equally acts on each particle and so accelerates the group rigidly as a whole, conserving its internal configuration.

The fact that dipole radiation selectively acts on the c.m. motion, while the Coulomb term affects only the relative configuration, renders effects of the electron-electron interaction unobservable with dipole radiation in parabolic confinements, where those degrees of freedom are completely independent. This is the basic message of the often-stated Kohn theorem. We would now like to focus on some rather obvious idea related to the Kohn theorem, which to some degree has appeared already several times in the literature (see, for example, Ref. 8), but seems to have not been fully exploited so far: the motion of a "superparticle."

Assume we put the $N$ electrons into the parabolic mesodot, starting from some random initial condition. Let there be friction forces, but no light field yet. As we have seen above, the particles spontaneously relax to a stable equilibrium configuration[29]—namely, the circular electron "lake" of radius $r_E$. In this situation, the c.m. will coincide with the potential minimum, $\vec{s} = \vec{0}$, and the internal configuration (resembling a Wigner crystal at low temperature) will be determined by a balance between repulsive Coulomb and compressive confinement forces.

If we now apply a proper electric field $\vec{E}$ as a control force, we can statically displace the lake from the $\vec{s} = \vec{0}$ position or dynamically move it around in the dot plane. All this will not change the internal configuration of the particles, as long as we take care not to leave the parabolic region.

The only way to disturb the shape of the lake is by applying different forces on each particle. Imagine, for simplicity, a single force kick on a specific electron $k$—for example, induced by a phonon scattering event—which instantaneously changes its velocity by an amount $\Delta\vec{v}_k$. The kicked particle will then start to move away from its specific relative position within the configuration. However, since it started from an equilibrium position, the particle will experience elastic restoring forces in the network of its neighbors. Note also that the term $[(m^\star\omega_0^2/2)(\vec{D}_k)^2]$ in Eq. (3) acts to pull particle $k$ back towards the momentary c.m. position of the lake. These conditions are schematically depicted in Fig. 8.

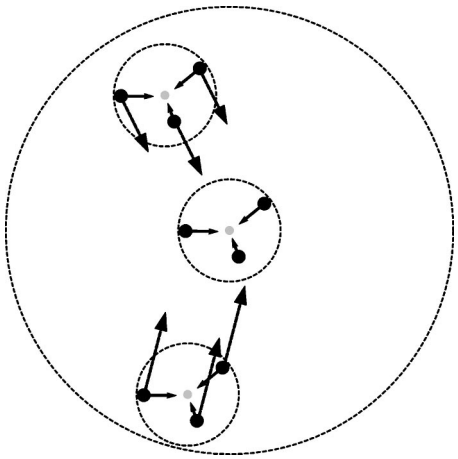

FIG. 8. Schematic of a superparticle (fine-dotted circles), consisting of three electrons (black dots), located at three different positions within a mesodot. The c.m. of the superparticle is represented by a small grey circle. The solid black arrows denote the "cohesive" forces, which in combination with the repulsive Coulomb forces tend to restore the size and inner configuration of the superparticle after deformation. The dashed arrows stand for the c.m. forces, acting on the superparticle as a whole and pulling it back to the center of the mesodot.

Therefore, with a little time delay, the momentum $\Delta\vec{p} = m^\star\Delta\vec{v}_k$ transferred from the phonon to particle $k$ will spread over the total $N$-electron system, leading to complex lattice vibrations of the Wigner crystal. In the limit of large particle numbers, this process may simply be viewed as a "heating" of the lake. But thanks to the gradual slowing down of the particles due to the friction force, this thermal energy will on the long run transfer to the semiconductor lattice and eventually be dissipated. As a result, the lake will restore its equilibrium shape within a view relaxation times $\tau$; i.e., it actually shows form-elastic behavior.[30]

For these reasons, it is natural to view the compact packet of $N$ electrons as a composite superparticle of formal mass $M = Nm^\star$ and charge $Q = Nq$ at the position of the c.m. When subject to an external homogeneous electric field $\vec{E}$, the superparticle reacts with an acceleration $\ddot{\vec{s}} = \vec{F}_{tot}/M = Q\vec{E}/M = q\vec{E}/m^\star$, the same as for an individual electron. Also most of the oscillator properties listed above [in particular, the eigenfrequency $\omega_0$ and the frequency-dependent amplitude $\Delta x(\omega)$] depend only on the ratio $Q/M = q/m^\star$ and thus remain unchanged. However, the polarizability $Q\Delta x/E_0$ of the superoscillator is $N$ times bigger than for a single particle. Note that when observed from a sufficient distance $r \gg r_E$, the Coulomb field of the superparticle will appear like that of a single giant charge $Q = Nq$.

Finally, let us discuss the effect of single-particle stochastic phonon scattering events on the orbit of the superparticle

as a whole. As a simple model for this diffusion process in the heat bath, assume that (besides the deterministic friction forces) the velocities $\dot{\vec{r}}_i$ of all particles are changed synchronously each time interval $\delta t$ by small, statistically independent random vectors $\Delta\vec{v}_i$. Let the directions of the increments be isotropic (angles equally distributed between 0 and $2\pi$) and their moduli be constant $|\Delta\vec{v}_i|=\Delta v_0$. Then, the total momentum transferred to the superparticle in one interval $\delta t$ is given by $\Delta\vec{p}_s=m^\star\Sigma_k\Delta\vec{v}_k$, corresponding to a velocity change of $\Delta\vec{v}_s=\Delta\vec{p}_s/M=(1/N)\Sigma_k\Delta\vec{v}_k$, which is also isotropic. Using complex numbers to represent the 2D vectors, $\vec{v}\leftrightarrow\tilde{v}=ve^{i\varphi}$ (where $v$ stands for the modulus and $\varphi$ for the phase of $\tilde{v}$), yields $\Delta\tilde{v}_s=(\Delta v_0/N)\Sigma_k e^{i\varphi_k}$ or $\Delta v_s/\Delta v_0=|(1/N)\Sigma_k e^{i\varphi_k}|$. The modulus of the random phasor sum on the right-hand side (RHS) of the last equation obeys a Rayleigh distribution with a mean value of $\langle\Delta v_s/\Delta v_0\rangle_{av}=\sqrt{\pi/(4N)}$. Consequently, the Brownian velocity fluctuations of the superparticle are suppressed by a factor $N^{-1/2}$ compared to the individual electron. In the limit of large particle numbers $N$ it will follow an almost deterministic trajectory, which justifies the simple incorporation of electron-phonon coupling in the form of an effective friction force. This feature is particularly useful for the coherent control of the superparticle by suitably shaped laser pulses.

We can thus summarize: When $N$ electrons with repulsive Coulomb interactions are placed into a parabolic confinement, they collectively form a superparticle of mass $M=Nm^\star$ and charge $Q=Nq$. It has a preferred shape and inner structure (the circular "Wigner lake" of radius $r_E$) and is stabilized in this form by elastic forces. If, in addition, each particle is subject to a friction force, the superparticle will restore its inner and outer equilibrium configuration after any deformation. This shape restoration and refocusing mechanism works independently from the present position of the c.m. of the superparticle, the motion of which can be selectively controlled by an external electric field $\vec{E}$. The stochastic velocity fluctuations of the superparticle c.m. are suppressed by a factor of $1/\sqrt{N}$.

### I. Interacting superparticles

We have seen above that the superparticle oscillates in a parabolic mesodot just like a single electron, yet with reduced Brownian noise. But there is another advantage, connected with its giant charge: The induced electric fields are $N$ times stronger and can thus provide Coulomb coupling between neighboring dots even at mesoscopic separations in the $\mu$m range.

For a quantitative analysis, we consider two mesodots with interdot distance $L$, placed at positions $\vec{R}_1=(0,0,0)$ and $\vec{R}_2=(L,0,0)$. Let the first dot have the design parameters $d$ and $N_D$ and a filling factor $f=N_E/N_D$. Its $N_E$-fold charged superparticle, resting in equilibrium at $\vec{R}_1$, produces at $\vec{R}_2$ an electric field $E^0_{ind}=N_E(k_0/q)/L^2$. If superparticle 1 is now shifted for some reason by an amount $\Delta x$, the induced change of electric field at $\vec{R}_2$ is $\Delta E_{ind}=[N_E(k_0/q)/L^3]\Delta x$. In particular, assume that we apply an external electric field $E_0$ to the system. As we have computed a little earlier, this shifts superparticle 1 by $\Delta x=qE_0/(m^\star\omega_1^2)$. We can insert this shift into the equation for $\Delta E_{ind}$ and calculate the ratio between the induced and external field at $\vec{R}_2$, which gives $\Delta E_{ind}/E_0=N_Ek_0/m^\star\omega_1^2L^3$.

In order to have a significant dynamic interdot Coulomb coupling, we require that this ratio should be comparable to unity or, at least, around 1/10. It is important to realize at this point that *the ratio is invariant under our scale transformation*—i.e., $(\Delta E_{ind}/E_0)\propto s^0$. Therefore, interacting dot arrays can be realized in the technologically convenient mesoscopic regime, despite the huge interdot distances. If we express the oscillator eigenfrequency by the design parameters of the doping ball model, $\omega_1^2=2\alpha/m^\star=N_Dk_0/(m^\star d^3)$, we obtain for the ratio the simple result $(\Delta E_{ind}/E_0)=f(L/d)^{-3}$.

In practice, $L$ must be at least as big as $2r_c=2\eta^{1/3}f^{1/3}d$ or, otherwise, the two electron lakes will merge. This yields, independently from the filling factor, $\Delta E_{ind}/E_0=1/8\eta$, so that coupling effects should indeed be observable. Note that the condition of two dots almost "touching" each other can be realized easily in the mesoscopic regime, but probably not with SAD's.

### J. Coupled modes

Our next goal is to compute the coupled modes of the two-dot system in the parabolic regime. The dots $i=1$ and $i=2$, placed along the $x$ axis at distance $L$, are characterized by the curvatures $2\alpha_i$ and the corresponding undisturbed eigenfrequencies $\omega_i$. They are occupied by $N_i$ electrons, which form superparticles with the total masses $M_i=N_im^\star$ and total charges $Q_i=-N_ie$.

Already without any external light field, the static Coulomb repulsion between the two superparticles leads to shifts of the in-plane equilibrium positions of the left particle from $\vec{r}_1=(0,0)$ to $\vec{r}_1'=\vec{r}_1+\delta\vec{r}_1=(0-\delta_1,0)$ and of the right particle from $\vec{r}_2=(L,0)$ to $\vec{r}_2'=\vec{r}_2+\delta\vec{r}_2=(L+\delta_2,0)$, so that the new effective interdot distance is $L'=L+\delta_1+\delta_2$. The static shifts $\delta_i$ are determined by the relation $2\alpha_1\delta_1=2\alpha_2\delta_2=N_1N_2k_0/(L')^2$, which yields a third-order polynomial equation for $\delta_1$.

The parabolic confinement potentials of the dots as a function of absolute superparticle positions $\vec{s}_i$ are $U_i(\vec{s}_i)=\alpha_i(\vec{s}_i-\vec{r}_i)^2$. In their new equilibrium positions $\vec{r}_i'=\vec{r}_i+\delta\vec{r}_i$, the superparticles are no longer at the minima $\vec{r}_i$ of their respective confinement potentials. However, this does not influence the effective confinement forces, as long as the parabolic region is not left. If we denote with $\Delta\vec{s}_i=(\Delta x_i,\Delta y_i)$, the relative displacement of superparticle $i$ from its new rest position—i.e., $\vec{s}_i=\vec{r}_i'+\Delta\vec{s}_i=(\vec{r}_i+\delta\vec{r}_i)+\Delta\vec{s}_i$–we find for a parabolic potential that $U_i(\Delta\vec{s}_i)=U_i^0+(2\alpha_i\delta\vec{r}_i)\Delta\vec{s}_i+\alpha_i(\Delta\vec{s}_i)^2$. The first term on the RHS is an irrelevant constant potential shift. The second term corresponds to a homogeneous electric field, which for small $|\Delta\vec{s}_i|$ is just exactly compensated by the Coulomb field of the other particle. The third term describes a parabolic confinement around the *new* equilibrium position, with the *same* curvature as before.

It is important to realize that this relaxation into a new global equilibrium configuration has a similar effect on the

two superparticles as the formation of the Wigner crystal had in each single dot: The purely repulsive Coulomb force between the superparticles is effectively transformed into that of a spring of relaxed length $L'$, which is still repulsive for $|x_1-x_2|<L'$, but becomes *attractive* for $|x_1-x_2|>L'$, at least with respect to the $x$ direction. On the other hand, if the superparticles are displaced in the $y$ direction, the Coulomb interaction is repulsive whenever $y_1$ differs from $y_2$. Keeping this in mind, we now proceed to determine the coupled modes of the system.

Our system has four degrees of freedom (labeled from now on by $k=1,\ldots,4$)—namely, the components of the relative displacements of the superparticles from their new rest positions, $\Delta\vec{s}_i=(\Delta x_i,\Delta y_i)$. We can thus define a four-dimensional vector $\vec{S}=(\Delta x_1,\Delta x_2,\Delta y_1,\Delta y_2)$ (note the capital $S$) which completely describes the spatial configuration of the two superparticles. Without friction, external light fields, and dynamic Coulomb interactions the equations of motion in these coordinates would read $M_k\ddot{S}_k=-2\alpha_k S_k$.

We next have to consider the total interaction energy $V(\vec{S})=N_1N_2k_0[(L'+S_2-S_1)^2+(S_4-S_3)^2]^{-1/2}$. For small deviations from equilibrium, we can expand this expression up to terms of second order in the form $V=V_0+\Sigma_k g_k S_k+(1/2)\Sigma_{mn}S_mA_{mn}S_n$, with the gradient $g_k=(\delta V/\delta S_k)_{\vec{S}=\vec{0}}$ and the Hess matrix $A_{mn}=(\delta^2V/\delta S_m\delta S_n)_{\vec{S}=\vec{0}}$. Then, the Coulomb forces are given by $\vec{F}_k^{coul}=-g_k-\Sigma_nA_{kn}S_n$. Note that the static $-g_k$ terms are exactly compensated by the parabolic confinement forces in equilibrium. The term $(-A_{kn}S_n)$ is the force acting on coordinate $k$, if coordinate $n$ is changed from zero to the value $S_n$. One finds that in the case of dots aligned along the $x$ axis, the Hess matrix is block diagonal and has the simple form

$$A_{kn}=\begin{pmatrix} +a & -a & 0 & 0\\ -a & +a & 0 & 0\\ 0 & 0 & +b & -b\\ 0 & 0 & -b & +b\end{pmatrix}, \tag{4}$$

with the two interaction parameters given by $a=+2N_1N_2k_0/(L')^3$ and $b=-N_1N_2k_0/(L')^3$ for the $x$ and $y$ directions.

Including the dynamic Coulomb forces into the equations of motion yields $M_k\ddot{S}_k=-2\alpha_kS_k-\Sigma_nA_{kn}S_n$. We insert the ansatz $S_k(t)=u_ke^{i\omega t}$ and obtain the eigenvalue problem $\Sigma_n[\omega_k^2\delta_{kn}+(A_{kn}/M_k)]u_n=\omega^2u_k$. Because of the block-diagonal matrix on the RHS, it can be solved separately for the two spatial directions. The equation for the $x$ direction reads

$$\begin{pmatrix}\omega_1^2+(a/M_1) & -(a/M_1)\\ -(a/M_2) & \omega_2^2+(a/M_2)\end{pmatrix}\begin{pmatrix}u_1\\ u_2\end{pmatrix}=\omega^2\begin{pmatrix}u_1\\ u_2\end{pmatrix}, \tag{5}$$

which is easily diagonalized. For the special case of equal electron occupations in both dots, $N_1=N_2=N$, one finds the following eigenfrequencies $\omega_{+,-}$ for the two coupled modes in $x$ directions:

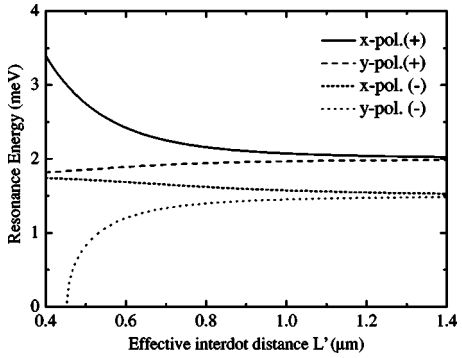


FIG. 9. Resonance frequencies $\hbar\omega_{(x,y)}^{(+,-)}$ of two Coulomb-coupled mesodots (hosting $N_1=N_2=1000$ electrons) as a function of the effective distance $L'$ between the superparticles, for light polarized in the $x$ and $y$ directions. The two mesodots are aligned along the $x$ axis. The uncoupled resonances are assumed at $\hbar\omega_1=2$ meV and $\hbar\omega_1=1.5$ meV, respectively.

$$\omega_{+,-}^2=\frac{\omega_1^2+\omega_2^2}{2}+\frac{a}{M}\pm\sqrt{\left|\frac{\omega_1^2-\omega_2^2}{2}\right|^2+\left(\frac{a}{M}\right)^2}. \tag{6}$$

For a special case, the eigenfrequencies of the coupled system have been plotted as functions of the effective distance $L'$ in Fig. 9 (see the solid and short-dashed curves). Without coupling ($a=0$, corresponding to the right side of the figure) the modes are at the undisturbed frequencies and correspond to independent oscillations of the two superparticles. With increasing coupling, both modes shift to the *blue*, with $\omega_-$ finally saturating at its upper limit $\sqrt{(1/2)(\omega_1^2+\omega_2^2)}$ and $\omega_+$ diverging. In the high-coupling regime, the $\omega_-$ mode corresponds to a pure c.m. motion (the superparticles oscillating in phase) and the $\omega_-$-mode to a relative motion (the superparticles oscillating out of phase). However, as we shall see later, all the oscillator strength will then be concentrated in the c.m. mode, so that the diverging relative mode is actually not observable for strong coupling.

The result for the $y$ modes is analogous (see the long-dashed and dotted curves in Fig. 9), however with the positive coupling parameter $a$ exchanged by the negative $b$. Therefore one obtains with increasing $|b|$ a shift to the *red* of these modes, with the c.m. mode (now given by $\omega_+$) approaching the limit $\sqrt{(1/2)(\omega_1^2+\omega_2^2)}$ from below and the relative mode becomes even softer. (At the critical coupling strength, where $\omega_-$ becomes 0, the system spontaneously polarizes already in the equilibrium configuration.) Only the c.m. mode is actually excitable with dipole light falling vertically on the double-dot system.

Finally, we address the question of how strong the coupling parameter $a$ has to be in order to get experimentally observable effects. To answer this, we confine ourselves to the special case of equal undisturbed oscillator frequencies, $\omega_1=\omega_2$. In the limit of small coupling we then consider the ratio of the Coulomb-induced frequency shift $(\omega_+-\omega_1)$ to the undisturbed resonance position $\omega_1$ and obtain $(\omega_+-\omega_1)/\omega_1=N_Dk_0/m^\star\omega_1^2L^3$. This is exactly the ratio $\Delta E_{ind}/E_0$, which we have computed above. We conclude again that the mesodots must be laterally close on a scale of $d$ for significant coupling.[31]

### K. Coherent control

Modern optical technology makes it possible to create (phase-locked sequences of) intense, ultrashort laser pulses in various frequency regimes and to shape their time-dependent electric field into almost any desired form.[32] When applied to a system of electrons, such shaped pulses act as electrical "steering forces" for the particles and can thus be used to coherently control their temporal evolution. For example, such techniques allow atoms to excite and stabilize quasiclassical Rydberg wave packets of electrons, which orbit at extreme distances from the nucleus with very small dispersion.[33] Alternatively, the ionization process of atoms can be controlled in a phase-sensitive manner with the correct choice of time-dependent light fields.[34] Even more spectacular experiments have been demonstrated in the field called "femtochemistry," where complex chemical reactions could be steered into a desired reaction pathway with various coherent control methods.[35] In these cases, one often had to use evolutionary pulse optimization to find the optimum light pulse shape. Of course, several coherent control experiments have been demonstrated with semiconductor nanostructures as well, and some of those were performed in the lower-frequency regime of intra-conduction-band transitions in which we are mostly interested here.[36]

As we have already pointed out in the Introduction, mesodots are particularly well suited for coherent control because of their tunable properties, low dispersion, and statistical stability of the superparticle and high polarizability of the corresponding oscillator. In addition, one can also think of more complex potential landscapes, tailor-made for the purpose of all-optical control of a many-electron system.

The simplest type of such experiments would be independent control of the stationary orbital radius $r_{orb}$ (or potential energy $E_{pot}=\alpha r_{orb}^2$) and velocity $v_{orb}$ [or kinetic energy $E_{kin}=(m^\star/2)v_{orb}^2$] of the superparticle. To achieve this, one has to choose the frequency of the exciting light force as $\omega=v_{orb}/r_{orb}$ and its amplitude as $F_{ext}=r_{orb}\sqrt{(2\alpha-m^\star\omega^2)^2+(2\gamma\omega)^2}$. Note that in the limit of small friction $\gamma\to 0$, resonant excitation will always lead to a situation with $E_{pot}=E_{kin}$. In order to establish, say, an orbit with large radius but small kinetic energy (below the optical phonon threshold), nonresonant excitation is required. In such an experiment, one could, for instance, drive the superparticle gradually out of the parabolic confinement regime and thereby excite its internal vibrational modes. The success of the control could be monitored by detecting coherently the emitted radiation of the accelerated supercharge.

Periodic orbits more complex than circles or ellipses and nonperiodic motions of the electron lake are also excitable with suitable light fields. If we treat phonon scattering in the approximative model of a velocity-dependent effective friction force, we can actually choose an arbitrary orbit $\vec{r}(t)$ for the superparticle, insert it into Newton's equation of motion, and directly compute the required light control force $\vec{F}_{ex}(t)=2\alpha\vec{r}(t)+2\gamma\dot{\vec{r}}(t)+m^\star\ddot{\vec{r}}(t)$. However, once the superparticle leaves the parabolic regime, it will start to disperse spatially and its control becomes much more demanding (and interesting).

An extreme departure of the superparticle from the potential minimum to beyond the binding region corresponds to an ionization of the mesodot. Another example of "femtochemistry" in semiconductor nanostructures would be the all-optical transfer of the superparticle from one mesodot to a close by neighbor. Using molecular dynamics simulations with up to 100 Coulomb interacting electrons in mesoscopic multidot potentials, we have simulated a transfer. It was found that such an experiment seems to be feasible with current techniques. However, these numerical results will be published separately in another paper.

## IV. SUMMARY AND OUTLOOK

In this paper we have proposed to use spatially selective doping techniques like the focused ion beam technique to create designable lateral potential landscapes within the plane of a quantum well. In the simplest case, this would be a rotationally symmetric potential minimum, termed a mesodot. Compared to self-organized quantum dots, typical mesodots have a very flat confinement potential and small resonance energies of the corresponding harmonic oscillator. They can host hundreds or thousands of electrons, which will at low temperatures form a confined, classical Wigner crystal of mesoscopically large radius. At somewhat higher temperatures the crystal will melt and form a "Wigner lake." It is dynamically characterized by center-of-mass coordinates and a large number of internal degrees of freedom.

Within the parabolic confinement regime, the electrons in the Wigner lake collectively respond to time-dependent dipole fields as a single superparticle of giant charge, which can be identified with the c.m. of the ensemble.

Random phonon scattering events of the individual electrons can temporarily disturb the inner configuration of the lake, but the combination of parabolic confinement forces and the electron's mutual Coulomb repulsion leads to an effective restoration mechanism. In addition, the Brownian fluctuations of the superparticle are statistically reduced compared to those of the constituent electrons. As a simple approximation, it may therefore be possible to describe the effect of the phonon collisions on the superparticle level as a deterministic, velocity-dependent friction force. Since the kinetic energies of the electrons can be kept below the optical phonon threshold in our mesoscopic system, it is possible to turn off the most critical decoherence mechanism in host semiconductors like, e.g., GaAs.

As a collective oscillator, the superparticle bound in a typical mesodot will have a high polarizability, due to the high charge and weak binding. Already with relatively weak continuous-wave excitation it can be driven on a mesoscopically large orbit, which could be monitored using the coherently emitted radiation of the accelerated charge. Also, the induced electric (near) field will be sufficiently strong to enable significant Coulomb coupling between neighboring mesodots, opening the way to arrays and more complex optically active systems. Furthermore, such designable potential landscapes would be ideally suited for coherent control experiments of various kinds. In particular, the superparticle can in principle be steered to follow any desired mesoscopic orbit, at least within the parabolic region.

For stronger (but feasible) optical excitation, the superparticle starts to probe the nonparabolic outer part of the lateral confinement potential, leading to various nonlinear effects. In this regime the superparticle's c.m. and internal degrees of freedom are no longer decoupled. This allows us, for example, to excite lattice vibrations of the Wigner crystal even with dipole radiation. At the same time, of course, the compactness of the superparticle will be lost and the Coulomb repulsion will cause dispersion. In the extreme case, the mesodot can be "ionized" partially or completely in a (coherently) controlled way. In particular, it should be possible to transfer a superparticle all optically from one mesodot to a close by neighbor. It would stay there for a long time in a metastable state (high potential barriers and mesoscopic spatial distances prevent a return to the first minimum by thermal or tunneling processes), until a second shaped optical pulse brings it back.

In order to further investigate the behavior of interacting groups of classical electrons in mesoscopic potential landscapes under the presence of phonon scattering, we have performed extended molecular dynamics simulations (to be published in a forthcoming paper), which theoretically confirm the above expectations. We hope that our article will also stimulate some experimental investigations in the proposed directions.


[1] T. Demel, D. Heitmann, P. Grambow, and K. Ploog, Phys. Rev. Lett. **64**, 788 (1990).

[2] S. Tarucha *et al.*, Phys. Rev. Lett. **77**, 3613 (1996).

[3] C. Sikorski and U. Merkt, Phys. Rev. Lett. **62**, 2164 (1989).

[4] A. Lorke, J. P. Kotthaus, and K. Ploog, Phys. Rev. Lett. **64**, 2559 (1990).

[5] M. Ciorga *et al.*, Phys. Rev. B **61**, R16 315 (2000).

[6] W. Kohn, Phys. Rev. **123**, 1242 (1961).

[7] P. A. Maksym and T. Chakraborty, Phys. Rev. Lett. **65**, 108 (1990).

[8] P. Bakshi, D. A. Broido, and K. Kempa, Phys. Rev. B **42**, 7416 (1990).

[9] Note that our "superparticle" is just a natural way of coarse graining from the level of individual electrons to groups of electrons confined to the same parabolic dot, which is perfectly justified for decoupled center-of-mass and relative coordinates. We do not want to imply by the term the formation of a "heavy fermion" in the sense of a new composite quasiparticle.

[10] This happens when $r_{orb}$ starts to exceed $r_{par}$. Thus, if the radius $r_E$ of the equilibrium electron lake in the mesodot is already comparable to $r_{par}$, only small electric forces are required to drive the border of the lake beyond the harmonic potential regime.

[11] The main scattering mechanism in many polar semiconductors. In GaAs this threshold is at about 36 meV.

[12] At this point, the superparticle concept can be used only as an approximation. In reality, the single-particle velocity that is relevant for the phonon emission is a vectorial sum of a center-of-mass part $v_{orb}$ plus a relative part, which depends on the internal motions of the superparticle's electrons. Only the c.m. part is controllable by the external dipole radiation. However, in the mesoscopic limit of large particle numbers and finite temperatures, the energies of the internal degrees of freedom will typically be of order $k_BT$. This electron temperature $T$ must be kept small enough in order to suppress LO phonon emission.

[13] B. N. Murdin *et al.*, Phys. Rev. B **55**, 5171 (1997).

[14] I. Banerjee and R. H. Livengood, J. Electrochem. Soc. **140**, 183 (1993).

[15] P. D. Prewett and G. L. R. Mair, *Focused Ion Beams from Liquid Metal Ion Sources* (J. Wiley, New York, 1991).

[16] J. Yanagisawa, T. Goto, T. Hada, M. Nakai, F. Wakaya, Y. Yuba, and K. Gamo, J. Vac. Sci. Technol. B **17**, 3072 (1999).

[17] S. Eshlagi, C. Meier, D. Suter, D. Reuter, and A. D. Wieck, J. Appl. Phys. **86**, 6605 (1999).

[18] D. Reuter *et al.*, Semicond. Sci. Technol. **18**, 115 (2003).

[19] K. Gamo, Microelectron. Eng. **32**, 159 (1996).

[20] We do not claim that our approach to fabricate mesoscopic dots by spatially selective doping is superior to any of the existing techniques. Our intention is to suggest an alternative method with certain useful features. Note that FIB doping is relatively simple from the processing point of view: No complicated etching or metallization is required. The latter point can be an advantage when FIR and THz experiments are considered. Metals can drastically affect the optical field distribution, but in our case the electrons are surrounded by dielectric material.

[21] At low temperatures and small doping concentrations, the impurity cluster in the doping ball will be in an "insulating state," with electron states localized at the individual donors. Thus there might occur a problem with the "freezing out" of carriers. However, note that in our proposed design the energy of the quantum well's ground subband is lower than the energies of the localized states in the doping ball. So in the thermal ground state the electrons should eventually end up in the well. In addition, it is possible in many applications to choose a rather high doping concentration $N_D$ (well above the Mott transition) and to slightly increase the spacer thickness $d$, so that the curvature of the parabolic potential remains constant

[22] FIB can only control the average local doping concentration, but of course not the atomic lattice positions of each individual impurity.

[23] The size quantization of the well must be sufficiently strong, so that the longitudinal ($z$-direction) and lateral ($x$-$y$ direction) electron dynamics can be separated and all relevant physics can be adequately described by considering the ground subband only.

[24] This is feasible since in practical devices the global electronic Fermi level $\Phi_E$ is pinned, for example by surface charges. With the electric tilting field of gate electrode, the subband edge of the longitudinal quantum well can be shifted relative to the Fermi level, thereby controlling the carrier density in the dot.

[25] C. Yannouleas and U. Landman, Phys. Rev. Lett. **85**, 1726 (2000).

[26] C. Yannouleas and U. Landman, Phys. Rev. B **68**, 035325 (2003).

[27] The coupled differential equations were solved with a fifth-order Runge-Kutta method

[28] Isolated means that there is no electron-phonon coupling (neither in the form of a deterministic friction force nor via stochastic

scattering events) and no perturbation by an external light field.

[29] More precisely, there are infinitely many equivalent equilibrium positions corresponding to different rotations around the center.

[30] Note that in combination with the parabolic confinement, the originally repulsive electron-electron interaction turns effectively into a springlike interaction. These "springs" have certain equilibrium lengths and react with linear restoring forces of both signs when they are slightly stretched or compressed.

[31] The accuracy of the distance should be, say, $1/10$ of the distance itself—i.e., of order $d/10$. In the mesoscopic regime, with $d$ in the range of several 100 nm, the required spatial accuracy is of order 10 nm, which is achievable with present FIB technology. (Note that due to the suppression of short-wavelength Fourier components of the Coulomb field due to the spacer layer, it is not neccessary to control the position of the individual doping atoms so precisely.) Thus, by shifting the length scale of our structures into the mesoscopic regime, their "accuracy margin" is also conveniently enlarged.

[32] A. M. Weiner, Rev. Sci. Instrum. **71**, 1929 (2000).

[33] H. Maeda and T. F. Gallagher, Phys. Rev. Lett. **92**, 133004 (2004).

[34] T. Weber *et al.*, Nature (London) **404**, 658 (2000).

[35] A. Assion *et al.*, Science **282**, 919 (1998).

[36] F. Eickemeyer *et al.*, Appl. Phys. Lett. **79**, 165 (2001).